Additional Information

Cortical somatostatin interneuron subtypes form cell-type specific circuits

Sherry Jingjing Wu[1,2,†], Elaine Sevier[1,2,†], Deepanjali Dwivedi[1,2], Giuseppe-Antonio Saldi[2], Ariel Hairston[1,2], Sabrina Yu[3,2], Lydia Abbott[4,2], Da Hae Choi[5,2], Mia Sherer[1,2], Yanjie Qiu[1,2], Ashwini Shinde[5,1], Mackenzie Lenahan[4,1], Daniella Rizzo[6,1], Qing Xu[7], Irving Barrera[2], Vipin Kumar[2], Giovanni Marrero[2], Alvar Prönneke[8], Shuhan Huang[1], Bernardo Rudy[8], David A. Stafford[9], Evan Macosko[2], Fei Chen[2], and Gord Fishell[1,2]

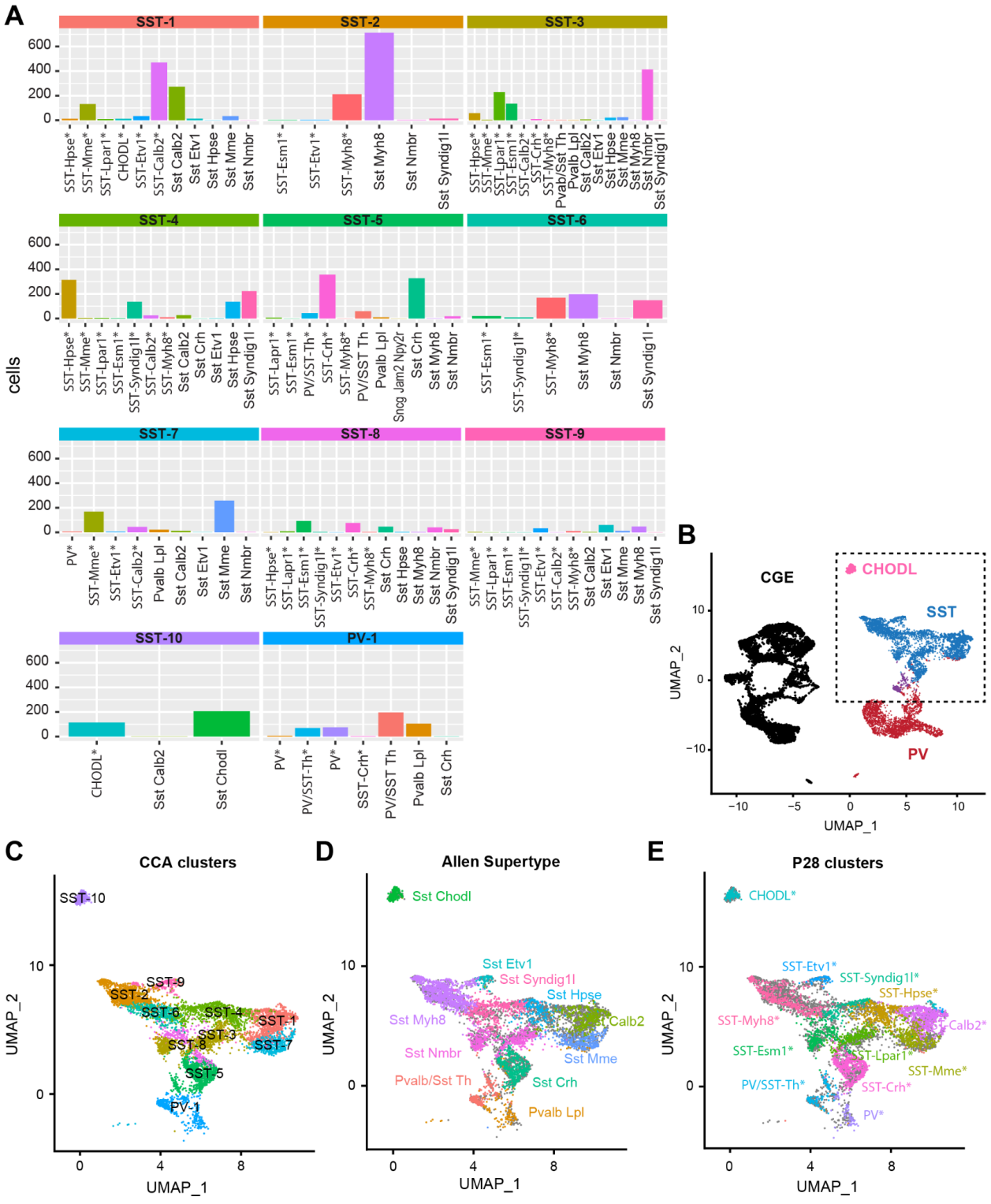

Figure A1. Label transfer from supertypes defined in Yao et al., 2021 to P28 SST interneuron clusters.

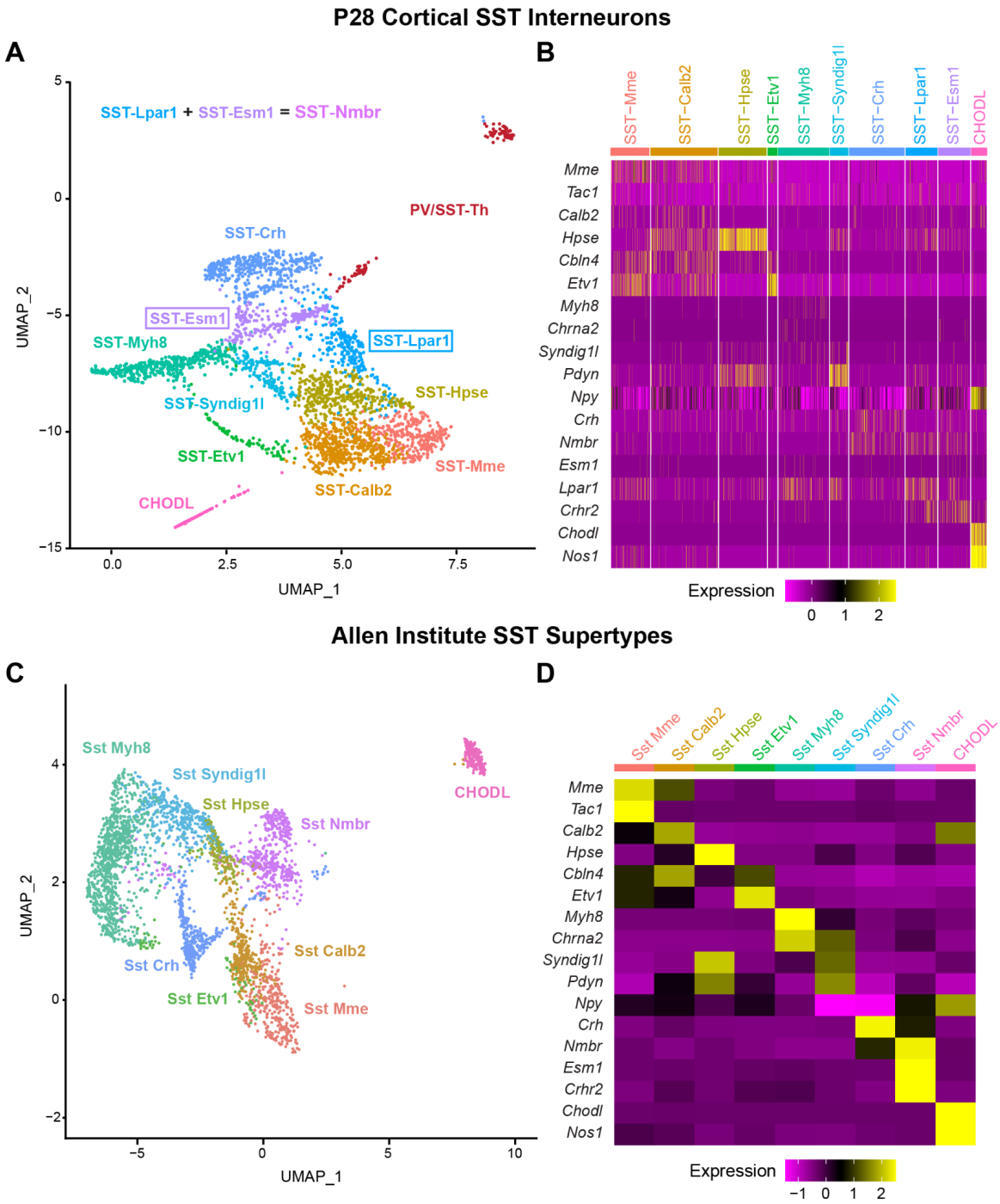

Figure A2. Marker gene expression of different SST subtypes in two datasets.

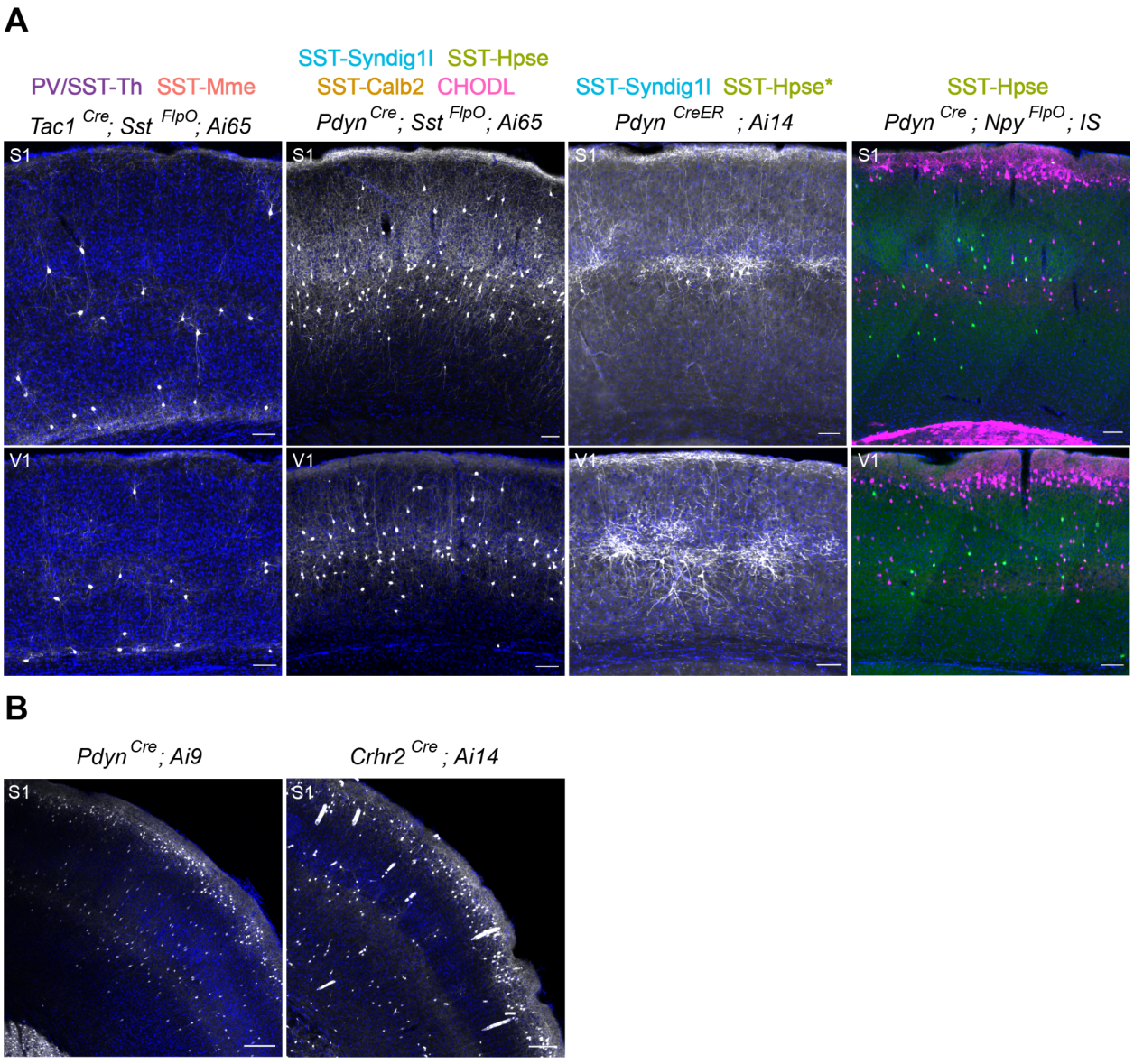

Figure A3. Labeling patterns of additional genetic strategies in S1 and V1.

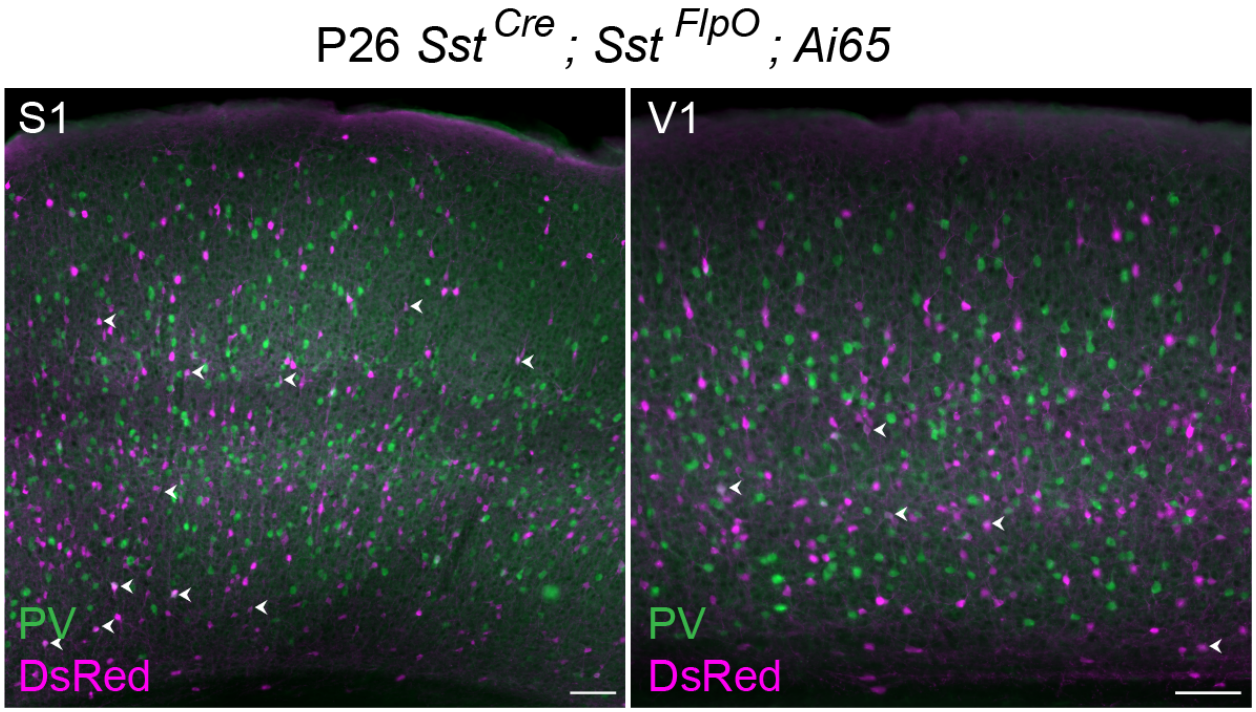

Figure A4. Intersectional genetic strategy Sst-Cre; Sst-FlpO; Ai65 does not label many PV+ interneurons. 3.25% of genetically labeled SST neurons were positive for PV in S1 (29/892 neurons), and 1.95% of genetically labeled SST neurons were positive for PV in V1 (17/873 neurons).

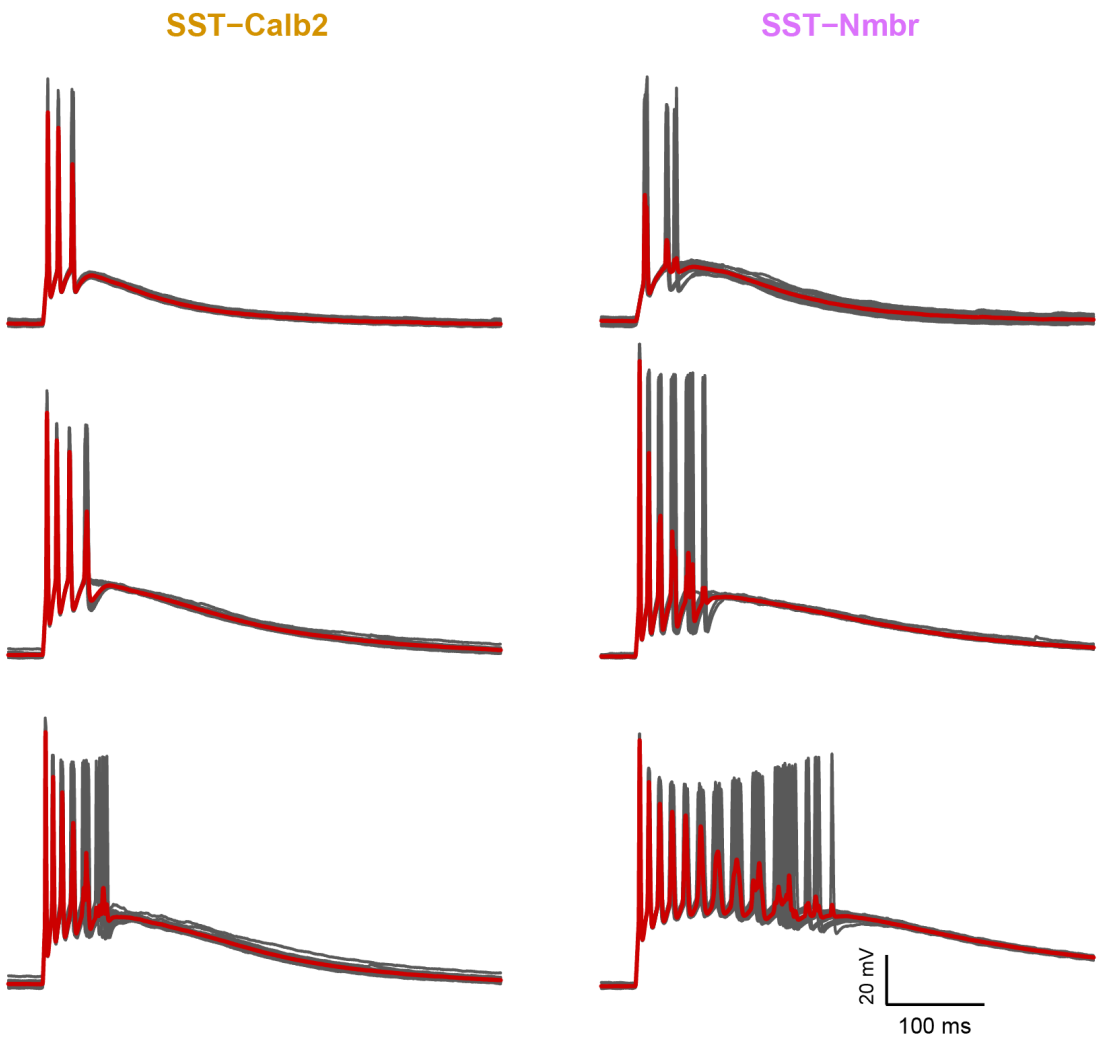

Figure A5. Optogenetic stimulation induces a variable number of spikes in SST interneurons.

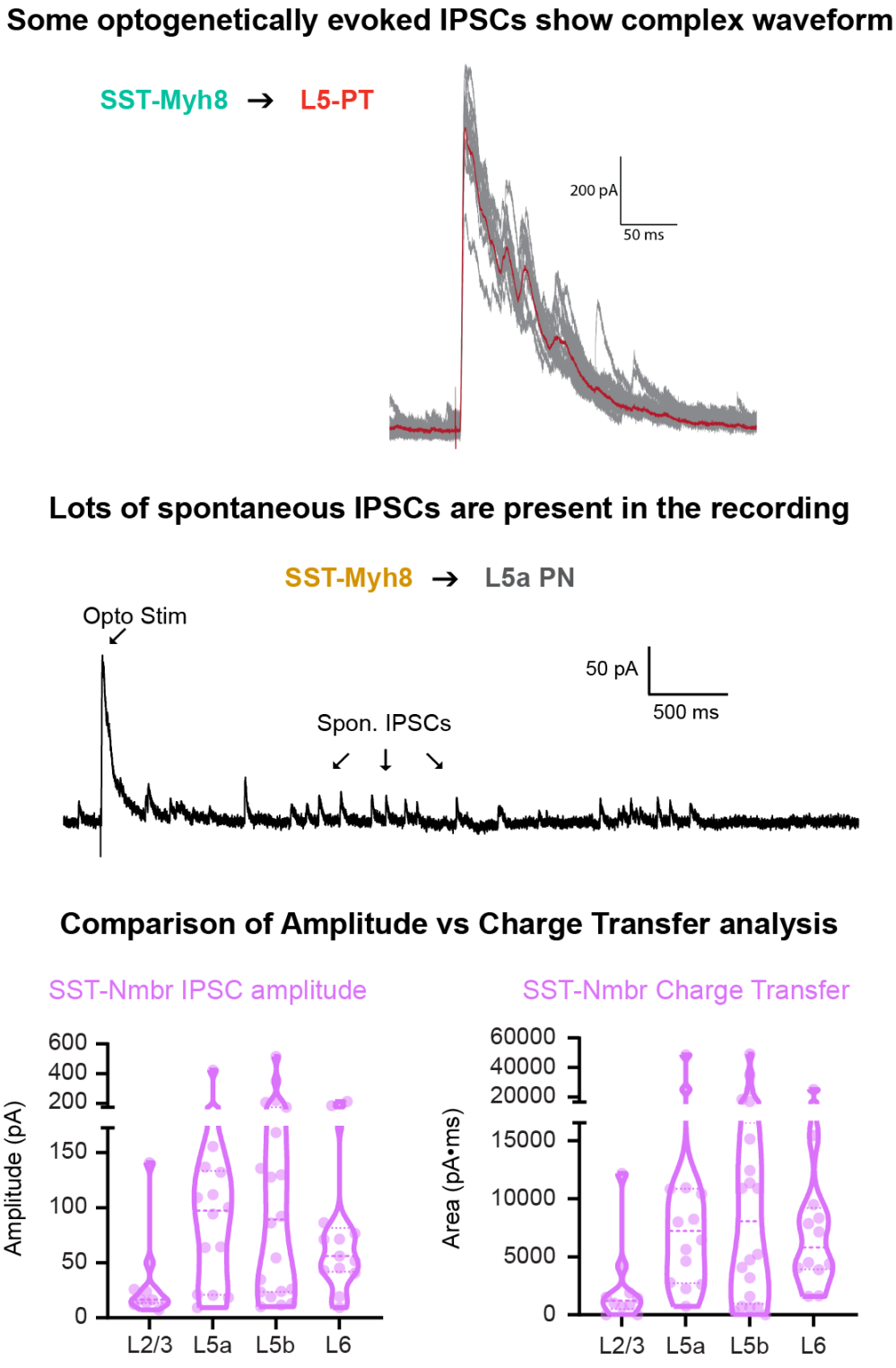

Figure A6. Some optogenetically evoked IPSCs show complex waveforms, making charge transfer analysis more variable than amplitude.

Example of membrane potential change in respond to optogenetic stimulation of SST-Calb2

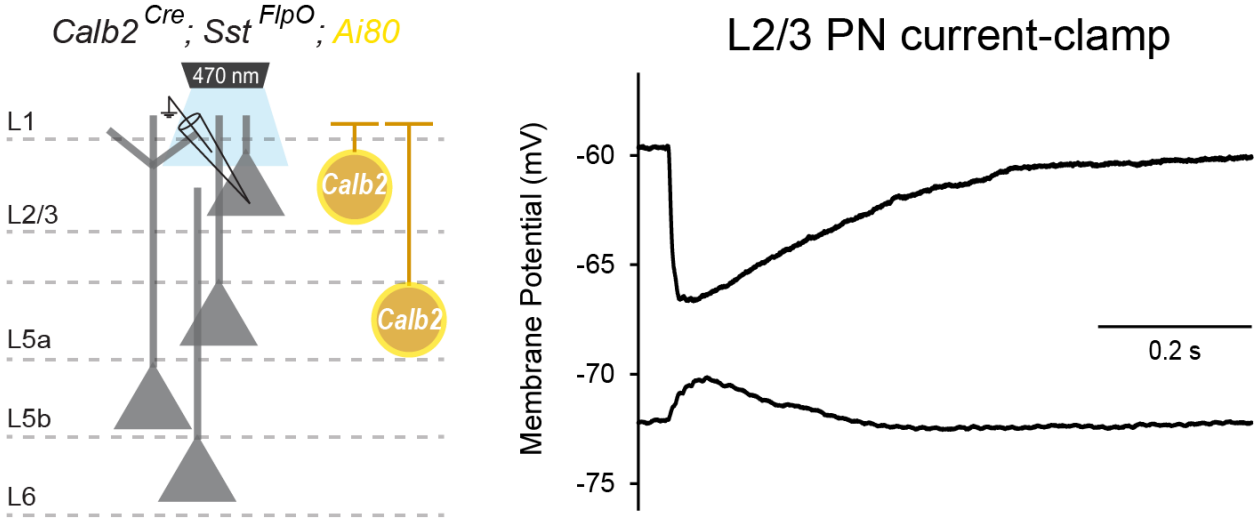

Figure A7. Optogenetic stimulation of SST-Calb2 interneurons drives the membrane potential of L2/3 pyramidal neuron towards chloride equilibrium potential.

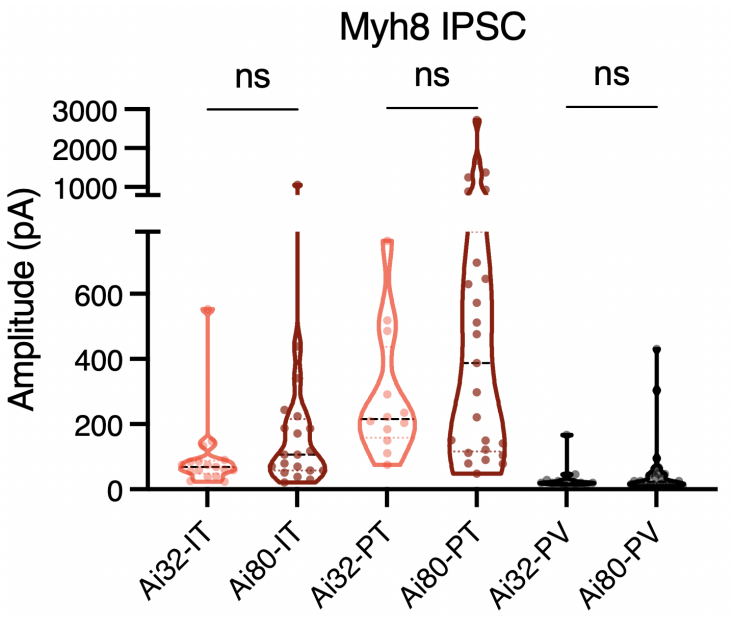

Figure A8. Two different channelrhodopsin reporter lines showed comparable results.

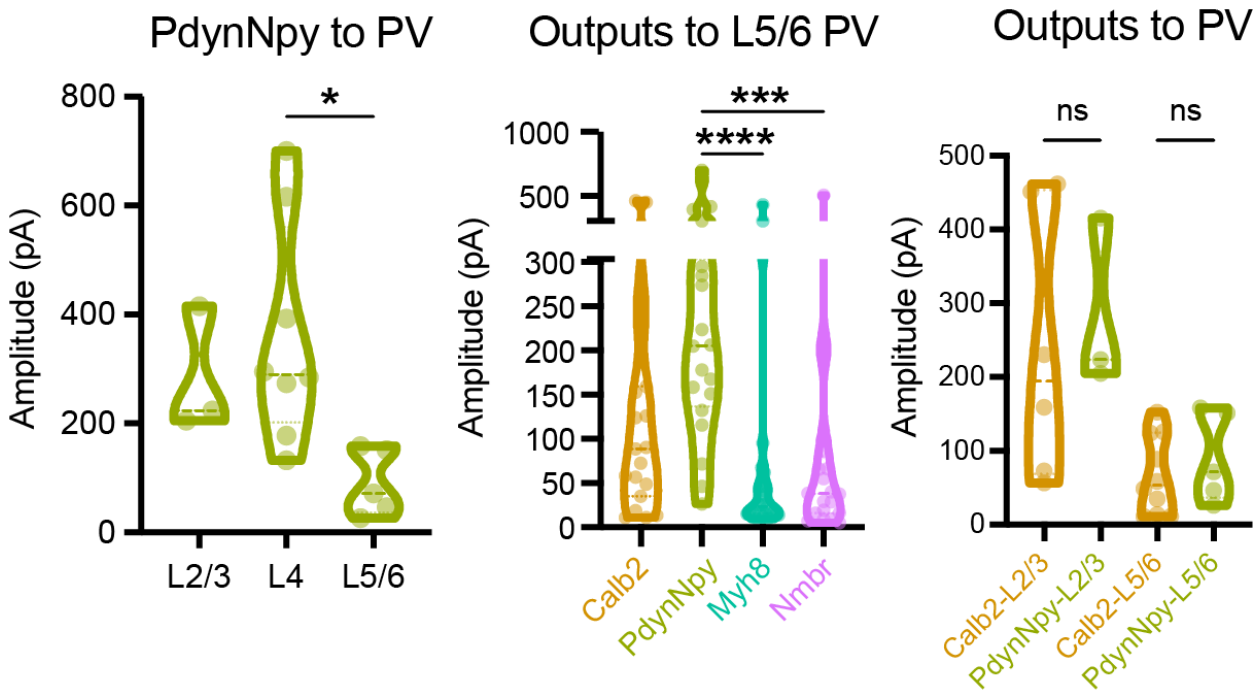

Figure A9. Pdyn;Npy labeled SST interneruons innervate L4 PV interneurons.

A. Violin plot of evoked IPSC upon stimulation of cells labeled with Pdyn-Cre;Npy-FlpO. IPSC in L4 PV interneurons was significantly greater than L5/6 PV interneurons ($p = .01$) by Kruskall-Wallis test with Dunn's correction.

B. Evoked IPSCs from all four SST types. SST-PdynNpy responses were signficantly greater than SST-Chrna2 ($p < .0001$) and SST-Crhr2 ($p = .0004$).

C. In L2/3 and L5/6, evoked IPSC from SST-Calb2 and SST-PdynNpy were not signficantly different ($p > .999$).

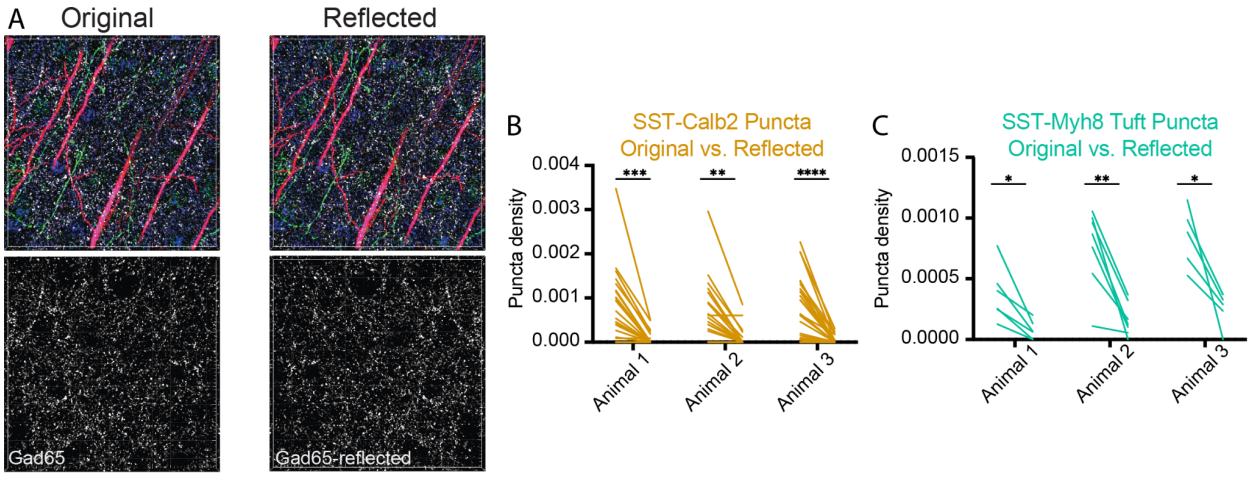

Figure A10. Synaptic puncta are detectable above noise levels.

A. Example images before (left) and after (right) reflecting the Gad65 channel.

B. Puncta density from Calb2 interneurons across all dendritic compartments before and after reflecting the Gad65 channel. Columns represent individual animals. Puncta density was significantly higher in the original images by multiple paired t-tests with Bonferroni-Dunn correction. CR-PT-1 $p = .0001$, CR-PT-3 $p = .0005$, CR-PT-6 $p < .0001$.

C. Same as in B but for Chrna2 puncta on tuft dendrites only. A-PT-7 $p = .035$, A-PT-8 $p = .006$, A-PT-9 $p = .047$.

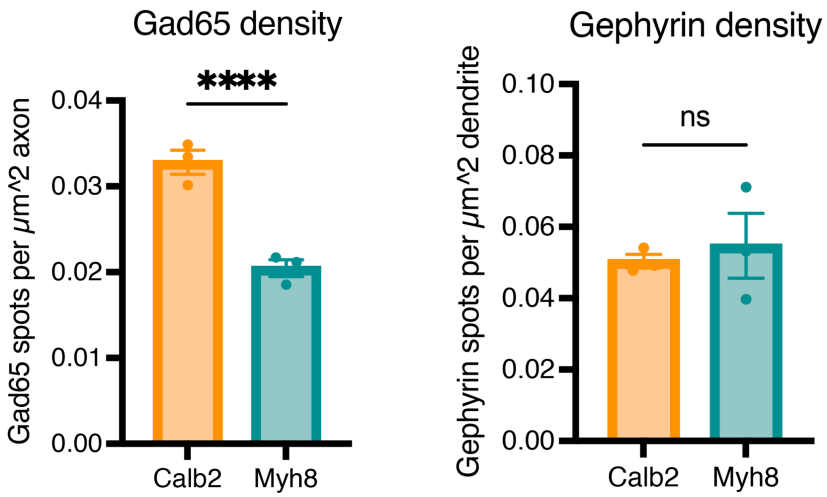

Figure A11. The density of Gad65 and Gephyrin immunolabeling for SST-Calb2 and SST-Myh8 on L5-PT neurons.